Thermal Protection of Ballistic Entry Vehicles

E. Arnold Reinikka* and Robert J. Sartell†

The Boeing Company, Seattle, Wash.

The concepts of radiation cooling and ablation cooling using char-forming plastic materials are examined for the purpose of providing thermal protection for ballistic vehicles entering the earth's atmosphere from near earth orbits. The effect on thermal protection requirements of re-entry from various orbit altitudes is presented. A general theory for charring ablation materials is discussed. Rapid means for calculation of aerodynamic heating encountered during ballistic re-entry are furnished. Design charts based on these data are included for determination of thermal protection weights when using ablation or radiation cooling. Weights are based on maintaining a controlled environment for the vehicle's interior and load-carrying structure.

Nomenclature

A = vehicle planform area, ft²
c_p = specific heat, Btu/lbm-°F
C_D = drag coefficient
D = diameter, ft
g = local acceleration of gravity, ft/sec²
H = heat-transfer coefficient based on enthalpy, lbm/ft²-sec
H_p = heat of pyrolysis, Btu/lbm
i = enthalpy, Btu/lbm
J = mechanical equivalent of heat, 778 ft-lbf/Btu
m = mass, slugs
$\dot{m}$ = mass loss rate, lbm/ft²-sec
$\dot{q}$ = heating rate, Btu/ft²-sec
r = recovery factor
r_c = radius of curvature, ft
R = radius, ft
T_d = decomposition temperature, °F
T = temperature, °F
t = time, sec
V = velocity, fps
W = vehicle weight, lbm
ρ = density, lbm/ft³
ψ = blocking function
γ = flight path angle, deg
ϕ = exponent involved in injection parameter
Γ = mass fraction of solid converted to gas, $\dot{m}_g/\dot{m}_s$
θ = cone half-angle, deg

Subscripts

a = air
e = edge of boundary layer
g = gas
I = inertial
0 = unblocked convective input
r = recovery
rel = relative
s = solid
sp = stagnation point
t = total.
w = wall
∞ = freestream condition

Introduction

VARIATIONS in entry missions and vehicle shape have a strong effect on heat shield requirements for ballistic entry vehicles. Rapid means for evaluating these requirements are desirable for preliminary design studies. In the past, various authors[1–5] have developed trajectory and heating data for ballistic entry vehicles based on an exponential atmosphere and on some simplifying approximations to the equations of motion. These methods provide a general knowledge of ballistic entry. Using these approximate methods, though, it is extremely difficult to evaluate 1) the effects of different initial velocities and flight path angles occurring when entering from various near-earth orbits (especially shallow entries); 2) the effects of ballistic coefficient on the flight path and total re-entry time; and 3) the effect of the actual atmosphere.

In the following text, trajectory and aerodynamic heating calculations are described for flight in a real atmosphere at various entry angles, and with a wide range of ballistic coefficients. An approximate analysis for char-forming ablators is presented. These calculations lead to: 1) the development of convenient normalized heating curves for evaluating aerodynamic heating when re-entering from near-earth orbits of up to 600 naut miles; and 2) design charts for determining thermal protection requirements for radiation and ablation cooled structures on ballistic vehicles.

Ablation Analysis

The complete mathematical description of the conservation of energy and mass during the ablation process of char-forming plastics requires consideration of such factors as reaction kinetics, the transport of thermal radiation through the material, char removal by combustion and/or rupture due to thermal stresses, the thermal equilibrium (or lack of it) between the gases and the char, and the transient effects due to heat storage.[6–10]

A relatively simple mathematical model is used in this ablation analysis. The material is divided into two regions, char layer and plastic, separated by a decomposition plane. The following assumptions are made.

1) All chemical reactions can be grouped into one single reaction that occurs at the decomposition plane with one overall heat of pyrolysis H_p (chemical reactions and radiation within the char are neglected).

2) The temperature range over which the reactions occur can be approximated by a single mean temperature T_d that remains constant during the ablation process.

3) Quasi-steady-state conditions exist. Thermal properties and Γ are constant.

The resulting equation for the energy balance in the char layer and the equations describing the ablation process are derived in Ref. 11.

The actual convective heat flux to the char surface during ablation is evaluated in the ablation analysis. The "blocking function" ψ is defined as the ratio of convective heat flux with mass injection to that without mass injection under otherwise identical conditions. The term $(1 - \psi)\dot{q}_0$ represents the re-

Received June 1, 1964; revision received September 18, 1964. The authors wish to express their appreciation to Norris Carver for preparation of the illustrations.

* Stress Analyst.

† Research Engineer.

duction in convective heating due to mass injection into the boundary layer. Studies indicate that, for most cases of interest, ψ depends primarily on the parameter $(c_{pg}/c_{pa})\phi\dot{m}_g \times (i_r - i_w)/\dot{q}_0$.

For turbulent flow, the blocking function curve recommended by Bartle and Leadon[12] for supersonic turbulent flow over a flat plate was used. The data of Ref. 13 were used for laminar flow. Both of these blocking functions are given in Ref. 11.

Trajectories

The flight path of a ballistic vehicle can be defined by 1) the initial entry angle and velocity and the vehicle's ballistic coefficient or 2) by specifying the circular orbit altitude, deorbit velocity applied to the vehicle when in orbit, and the vehicle's ballistic coefficient. The latter method is equivalent to the first, since each deorbit velocity produces a specific entry angle and velocity relationship.

The studies described in this report are based on the assumptions that initial entry occurs at an altitude of 400,000 ft, the vehicle is a point mass, the trajectory lies in a single plane, the earth is spherical, drag is independent of Mach number, wing loading remains constant during entry, and the Air Research and Development Command 1959 atmosphere applies.

The entry conditions utilized in this study for entry from various circular orbit altitudes are presented in Fig. 1. These data are based on firing the deorbit retrorocket at an angle relative to a vehicle's flight path which produces the maximum entry angle for a specific deorbit velocity. This criterion insures minimum total system weight when entering at a specific entry angle.

The flight path for ballistic vehicles is described by the following equations:

$$\frac{mV_I^2}{r_c} - mg\cos\gamma - mV_I\frac{d\gamma}{dt} = 0 \qquad (1)$$

$$C_DA\frac{\rho_\infty}{2}V_{\mathrm{rel}}^2 + mg\sin\gamma - m\frac{dV}{dt} = 0 \qquad (2)$$

Solutions of these equations are presented in Fig. 2 for entry from various orbit altitudes with various ballistic coefficients.

Solving Eq. (2) for flight time gives

$$t = \frac{1}{g\sin\gamma}\int_{V_1}^{V_2}\left[1 + \frac{C_DA}{w}\frac{\rho_\infty V_{\mathrm{rel}}^2}{2\sin\gamma}\right]^{-1}dV \qquad (3)$$

This shows that the time of flight along ballistic flight paths is a function of the initial entry angle. It should be noted that the integration shown is valid only when the flight path angle remains constant and is approximately valid when the flight path angle does not change significantly from the initial entry angle.

Aerodynamic Heating

Re-entry vehicles generally experience two modes of aerodynamic heating, convective and radiative. For entry from near-earth orbits, thermal radiation from the hot shock layer is negligible compared with the heating by convection for all but extremely high entry angles or ballistic coefficients; therefore, only convective heating is considered in this study.

When defining the heating history of a vehicle during reentry it is convenient to work with "cold wall heat flux" Hi_r rather than the actual heat flux $H(i_r - i_w)$ because the wall enthalpy i_w can vary considerably with time and position on a vehicle. The heat-transfer coefficient H can be considered independent of wall temperature with very little error. Since the recovery enthalpy is essentially a function of velocity and altitude, Hi_r can be assumed independent of wall temperature and thus of the heat shield material and thermal protection concept being used. Therefore, for a particular vehicle configuration, location on a vehicle, and type of flow (i.e., laminar or turbulent) the cold wall heating rate is assumed to be a function of altitude and velocity only.

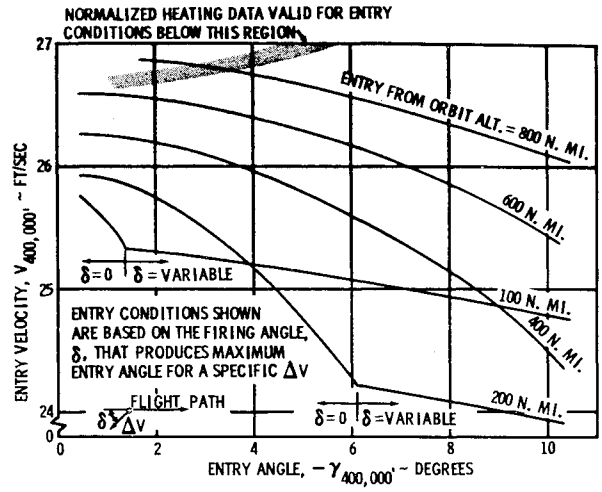

Fig. 1 Re-entry conditions for deorbit from various orbit altitudes.

Variations in entry angle and ballistic coefficient produce many different altitude-velocity profiles and different total flight times. These variations produce significantly different thermal environments. As a result, preliminary design studies are very tedious and time consuming if a large variety of vehicle configurations and entry conditions must be considered, since it is necessary to determine the time history of heating at a number of locations on a given vehicle in order to calculate the total heat shield weight.

Normalized Heating Curves

Rather than consider each flight profile for each vehicle as a separate case, it has been found that the use of normalized heating curves greatly reduces the time and effort required for the preliminary design analysis of ballistic vehicles. The time histories of cold wall heat flux ($\dot{q} = Hi_r$) incident on vehicles flying different ballistic flight paths when re-entering from near earth orbits result in similar shaped curves with the absolute value of entry time and heating rate dependent on entry angle, entry velocity, and W/C_DA. Entry angle and velocity affect both the maximum heating rate encountered and total flight time, whereas the ballistic coefficient principally affects the value of the maximum heating rate. Normalizing the cold wall heat flux encountered in flying the different trajectories, i.e., determining $(Hi_r)/(Hi_r)_{\max}$, and

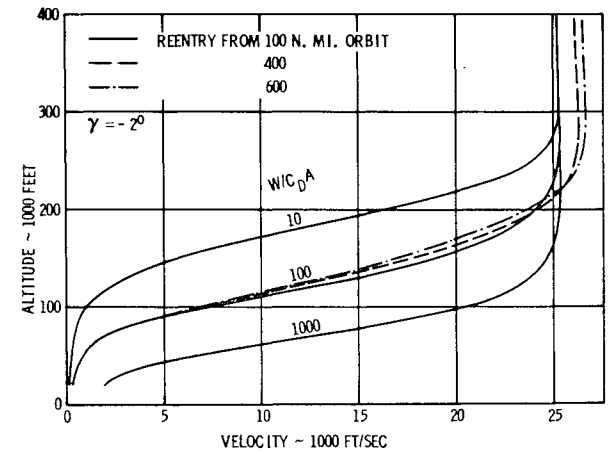

Fig. 2 Ballistic trajectories.

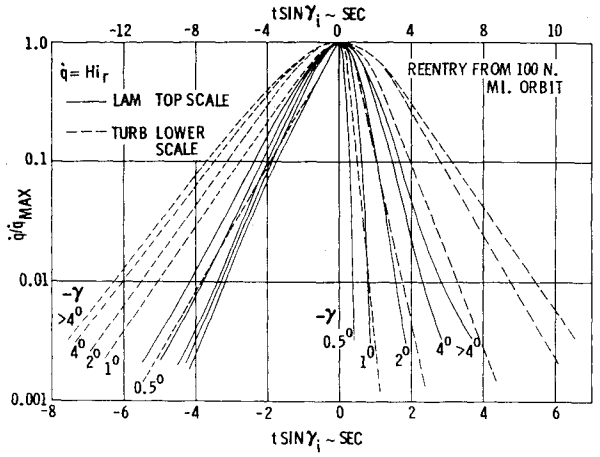

Fig. 3 Normalized heat pulses, laminar and turbulent flow.

plotting this ratio vs $t \sin\gamma$, results in the heating data for entry from a given orbit altitude at angles greater than 4° being approximated by a single curve. Entry at angles less than 4° results in separate curves for each entry angle. The normalized curves for laminar and turbulent flow are different and are shown in Fig. 3 for entry from a 100 naut mile orbit.

In order to use the normalized heating rate curves to conduct detailed thermal analyses, the curves for normalized recovery enthalpy and heat-transfer coefficient, $i_r/i_{r\,\text{at}\,\dot{q}_{\max}}$ and $H/H_{\text{at}\,\dot{q}_{\max}}$, are required. Recovery enthalpy is defined by

$$i_r = i_e + (rV_e^2/2gJ) \tag{4}$$

which, for the stagnation point of a body, is

$$i_{r,sp} = i_t = i_\infty + (V_\infty^2/2gJ) \tag{5}$$

Within the principal heating regime in the earth's atmosphere (altitude $\leq$ 300,000 ft), the total enthalpy i_t can be approximated by

$$i_t = 100 + (V_\infty^2/50{,}000) \text{ Btu/lbm} \tag{6}$$

The normalized heat-transfer coefficient can then be determined by

$$\frac{H}{H_{\text{at}\,\dot{q}_{\max}}} = \frac{\dot{q}/\dot{q}_{\max}}{i_r/i_{r\,\text{at}\,\dot{q}_{\max}}} \tag{7}$$

where

$$\frac{i_r}{i_{r\,\text{at}\,\dot{q}_{\max}}} = \frac{100 + V_\infty^2/50{,}000}{100 + V_\infty^2{}_{,m}/50{,}000}$$

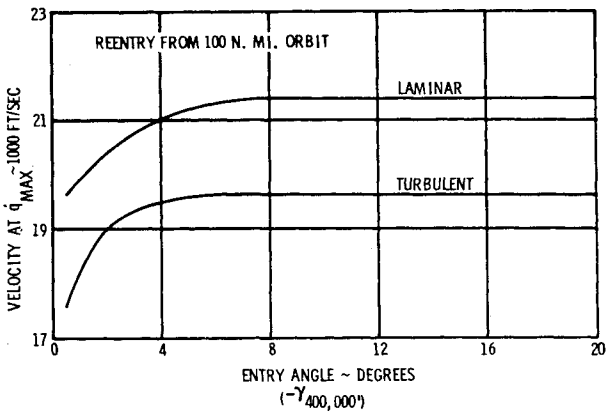

Fig. 4 Velocity at $\dot{q}_{\max}$, laminar and turbulent flow.

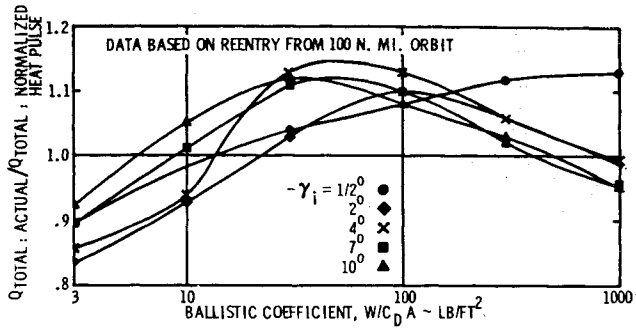

Fig. 5 Effect of ballistic coefficient on total heat, laminar flow.

$V_{\infty,m}$ is the velocity at $\dot{q}_{\max}$ and is given in Fig. 4 for entry from a 100-naut-mile orbit.

As stated previously, variations in ballistic coefficient primarily affect the value of $\dot{q}_{\max}$. However these variations also affect re-entry time and thus the total heat encountered, i.e., $\int(\dot{q}/\dot{q}_{\max})dt$. This effect is shown for laminar flow in Fig. 5. This shows that there is a maximum variation of about 15% in the total "cold wall" heating. This variation produces considerably smaller variations in total thermal protection requirements. Thus the assumption that W/C_DA affects $\dot{q}_{\max}$ only is justified for preliminary design studies.

The normalized heating data of Fig. 3 are all for entry from a 100-naut-mile orbit. For certain entry angles, normalized heating curves for entry from higher orbit altitudes are similar in shape to those for 100 naut miles; thus the curves for 100 naut miles apply. Such entry velocity-entry angle relationships are given in Fig. 1. The primary effect of greater orbit altitude is to increase the entry time and thus the total heat input. The variation in total heat, $\int(\dot{q}/\dot{q}_{\max})dt$, with orbit altitude is given in Fig. 6. These data show that the effect of orbit altitude is greatest for small entry angles.

Effect of Entry Direction

The normalized heating data presented are based on polar entry; however, entry from the east or west has a very small effect on the normalized heat pulse. The initial entry velocity change of ±1500 fps changes the total entry time by only a few seconds. For instance, for entry at $\gamma = -2°$ from a 100-naut-mile orbit with $W/C_DA = 100$ lb/ft², the time to reach an altitude of 20,000 ft varies by only 3 sec between eastward and westward entry. Entry direction then influences only the maximum value of cold wall heat flux and not the normalized heat pulse.

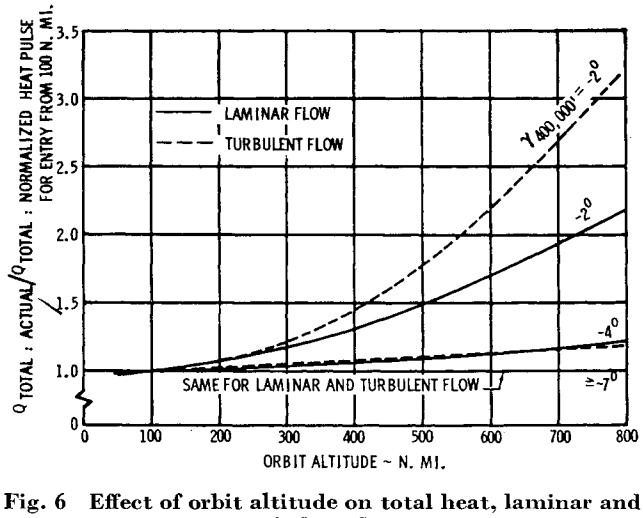

Fig. 6 Effect of orbit altitude on total heat, laminar and turbulent flow.

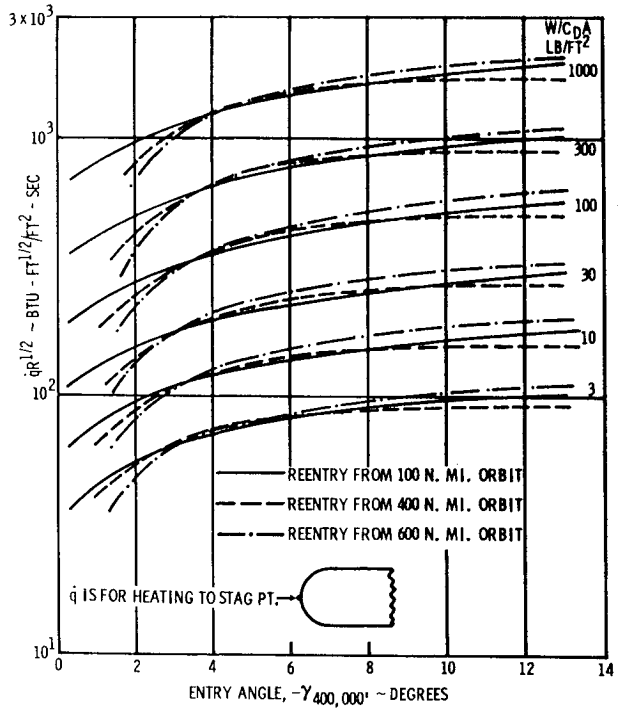

Fig. 7 Maximum heating rate, laminar flow.

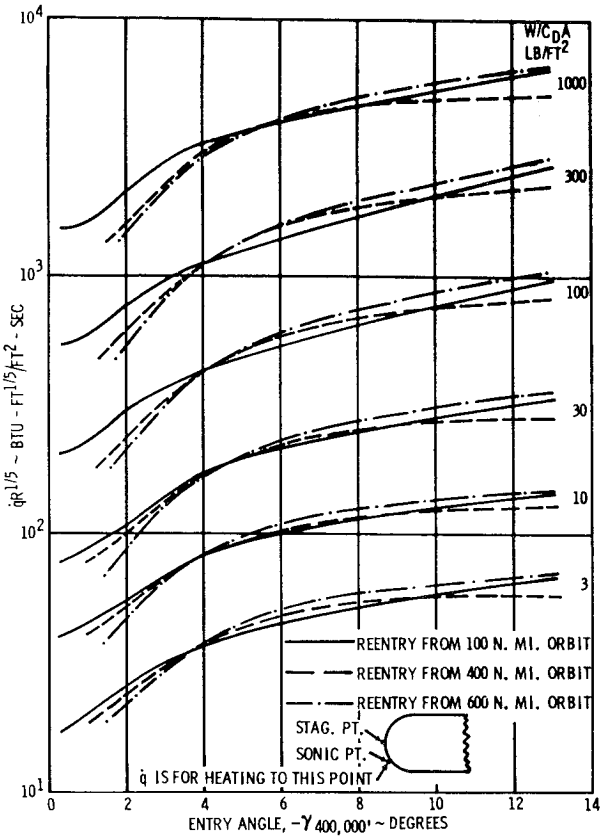

Fig. 8 Maximum heating rate, turbulent flow.

Maximum Heating Rates

In order to use the normalized heating curves, the maximum heating rate $\dot{q}_{max}$ must be known. Values of $\dot{q}_{max}$ are presented in Figs. 7 and 8 for laminar and turbulent flow, respectively, as a function of entry angle and ballistic coefficient for entry from 100-, 400-, and 600-naut-mile orbits. The laminar data are for spherical stagnation point, whereas the turbulent data are for the sonic point of a sphere. The laminar data are based on the theory of Fay and Riddell.[14] The theory of Van Driest[15] was used for the turbulent values.

Design Charts

The normalized heating curves in Fig. 3 were used to develop design charts for rapid determination of thermal protection requirements on ballistic vehicles entering from near-earth orbits. Thermal protection weights were evaluated as a function of entry angle and $\dot{q}_{max}$ since, as shown in the normalized curves, these parameters define the time history of re-entry heating. The normalized heating curves were modified to include a realistic landing condition consisting of a parachute descent from an altitude of 20,000 ft. This was necessary to produce reasonable results since the backside temperature reaches a maximum toward the end of flight. This is due to the finite time required to dissipate heat stored in the ablation or insulation materials.

Ablation and radiation thermal protection concepts that were evaluated are shown in Fig. 9. Ablation cooling can be utilized on the entire vehicle, whereas radiation cooling is limited to areas of relatively low maximum heating rate. The ablation concept consists of ablation material bonded to aluminum structure. The ablation material utilized is microballooned phenolic nylon. Properties of this material are given in Ref. 11. The radiation concept consists of refractory tiles supported by tubular members with Q-felt or zirconia insulation between the tiles and the water-cooled aluminum structure. The thermal protection weights are based on a maximum aluminum temperature of 200°F. The aluminum structure is considered insulated (no heat flows into the interior).

Thermal protection weights per unit area are shown in Fig. 10a for the ablation concept. The weights are given as a function of maximum cold wall heating rate for 1) entry angles ranging from -0.5° to −20°, and 2) for entry from orbit altitudes of 100, 400, and 600 naut miles. The items comprising the total thermal protection weight for entry from a 100-mile orbit are shown in Figs. 10b and 10c.

The ablation weights are based on: 1) factors of 1.25 for material ablated and 1.0 for material remaining for insulation and 2) a maximum allowable char thickness of 0.25 in.

As stated previously, the ablation analysis used for this study accounts for the actual ablation mechanism and char removal in a simplified manner. Recent calculations using a newly developed transient ablation computer program (based on the theory of Ref. 8) yielded thermal protection weights which were 20–30% greater than those presented

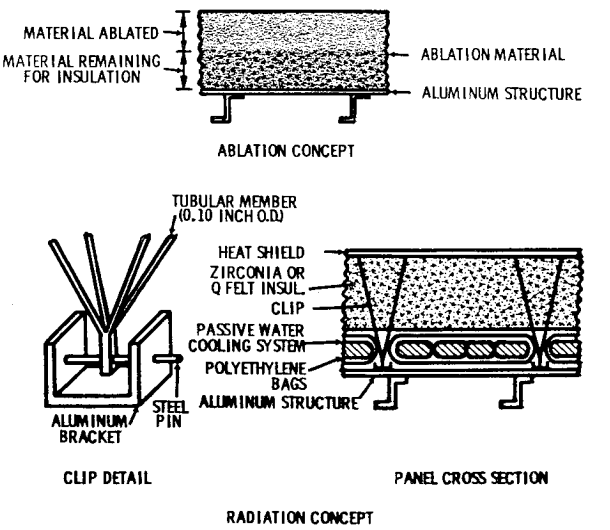

Fig. 9 Thermal protection concepts.

herein (Fig. 10a). Entry angles of $-0.5°$ and $-10°$ were considered for a 100-naut-mile orbit. A comparison between the results of the two theories is given in Table 1. These data indicate that the ratio of thermal protection weights resulting from the two theories is approximately constant over the range of entry conditions considered.

The data in Fig. 10a show that total entry time, which is proportional to $\sin\gamma$, has a much larger effect on total thermal protection weight than variations in $\dot{q}_{max}$, and that, as orbit altitude increases, thermal protection weights increase considerably at the low entry angles. This reflects the higher total heat inputs shown in Fig. 6. Weights for $\gamma = -0.5°$ are shown for entry from a 100-naut-mile orbit only. A ballistic vehicle would skip at this angle (not stay in the atmosphere in the first pass) when returning from the higher orbit altitudes.

Thermal protection weights for the radiation concept are presented in Fig. 11 for entry from a 100-naut-mile orbit. Weights for the ablation concept are also shown for comparison. The radiation weights are based on use of a passive water wall and 4.5 lb/ft³ Q-felt insulation behind the Rene 41 and molybdenum heat shields, and 8 lb/ft³ zirconia fiber insulation behind the tantalum heat shield. As shown, radiation cooling is only competitive "weight wise" at $\gamma = -0.5°$ and $\dot{q}_{max}$ up to 60 Btu/ft²-sec. Thus, radiation cooling does not appear very practical on any part of a ballistic vehicle.

Two other radiation structural concepts were investigated (see Fig. 12). Concept *C* was found to be the lightest. Utilization of this concept would extend the range of entry angles to $\gamma = -2°$ where radiation is competitive with ablation cooling.

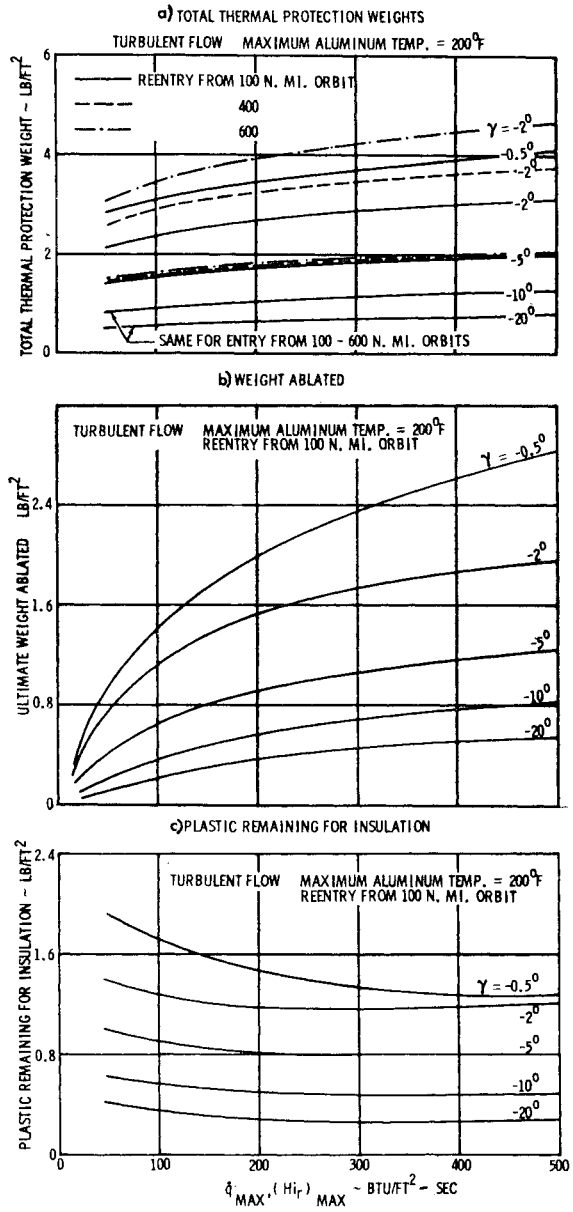

Fig. 10 Thermal protection system and component weights.

Application

The normalized heating curves and design charts were used to determine thermal protection requirements for three

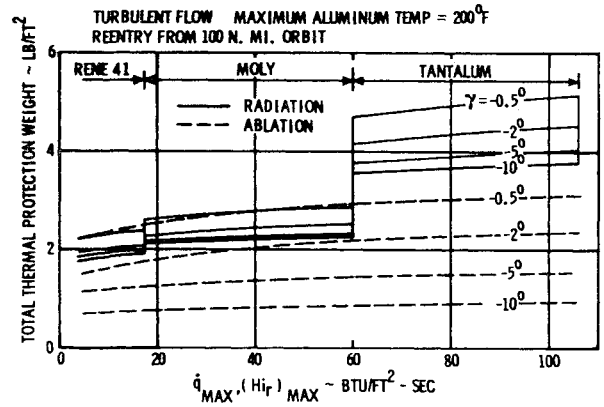

Fig. 11 Comparison of ablation and radiation cooling.

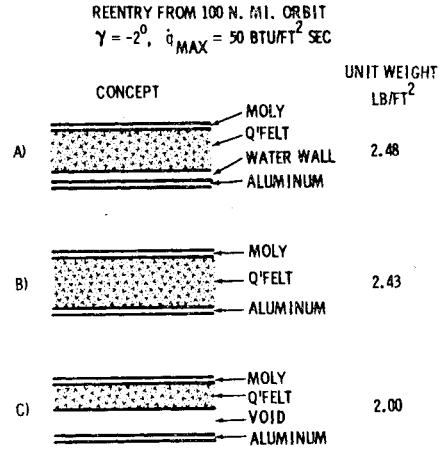

Fig. 12 Comparison of radiation cooling structural concepts.

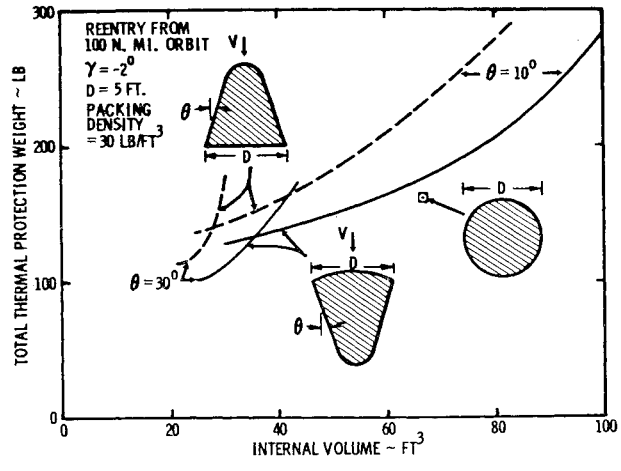

Fig. 13 Thermal protection of various ballistic shapes.

Table 1 Comparison of results of different ablation theories

γ	$\dot{q}_{max}$	Total thermal protection weight, psf: Simplified analysis	Total thermal protection weight, psf: New program
−0.5°	50	2.8	3.4
−0.5°	200	3.5	4.5
−0.5°	500	4.1	5.1
−10°	50	0.85	1.1
−10°	200	1.1	1.3
−10°	500	1.25	1.5

ballistic entry configurations: spheres, blunt cones, and inverted blunt cones (Apollo type) (see Fig. 13). The diameter D was held constant and the internal volume was varied by changing the length of the vehicle and thus the cone tip diameter. The cone half-angle θ was varied from 10° to 50°. As shown in Fig. 13, a spherical shape results in the lowest weight for a specific volume requirement. Exclusive of the sphere, the Apollo-type shape with a half-angle of 10° resulted in the lowest weight for the vehicles considered.

Conclusions

1) A convenient method for determining convective heating rates to ballistic vehicles returning at various entry angles from circular orbit altitudes of up to 600 naut miles is presented.

2) Design charts for determining thermal protection weights for radiation cooled and char-forming ablation-cooled structures were developed. The charts for ablation cooling were based on a simplified ablation theory and estimated material properties for microballooned phenolic nylon. The same techniques could be applied with other materials with the same or a more refined ablation theory. Recent calculations using a newly developed transient ablation program yielded thermal protection weights 20–30% greater than those given by the design charts.

3) Total thermal protection weights for several ballistic entry configurations are presented and compared. It is concluded that, for shapes other than spheres, the Apollo-type configuration is the lightest for a given internal volume.

References

[1] Chapman, D. R., "An approximate analytical method for studying entry into planetary atmospheres," NASA TR R-11 (1959).

[2] Allen, J. J. and Eggers, A. J., Jr., "A study of the motion and aerodynamic heating of missiles entering the earth's atmosphere at high supersonic speeds," NASA Rept. 1381 (1958).

[3] Gazley, C. Jr., "Deceleration and heating of a body entering a planetary atmosphere from space," Rand Rept. P-955 (1957).

[4] Hankey, W. L., Jr., Neumann, R. D., and Flinn, W. H., "Design procedures for computing aerodynamic heating at hypersonic speeds," Wright Air Development Center TR 59-610 (June 1960).

[5] Brunner, M. J., "Analysis of the aerodynamic heating for a reentrant space vehicle," J. Heat Transfer **81**, 223–229 (August 1959).

[6] Scala, S. M. and Gilbert, L. M., "Thermal degradation of char-forming plastics during hypersonic flight," ARS J. **32**, 917–924 (1962).

[7] Swann, R. T. and Pittman, C. M., "Numerical analysis of the transient response of advanced thermal protection systems for atmospheric re-entry," NASA TN D-1370 (1962).

[8] Munson, T. R. and Spindler, R. J., "Transient thermal behavior of decomposing materials, Part 1: General theory and application to convective heating," IAS Preprint 62-30 (January 1962).

[9] Lafazan, S. and Siegel, B., "Ablative thrust chambers for space application," American Institute of Chemical Engineers, Preprint 5 (February 1962).

[10] McFarland, B., Joerg, P., and Taft, M., "Criteria for plastic ablation materials as functions of environmental parameters; Part 1: Results of analytical studies," Tech. Doc. Rept., Aeronautical Systems Div. TR-61-439 (May 1962).

[11] Reinikka, E. A. and Wells, P. B., "Charring ablators in lifting entry," AIAA Preprint 63–181 (June 1963).

[12] Bartle, E. R. and Leadon, B. M., "The effectiveness as a universal measure of mass transfer cooling for a turbulent boundary layer," *Proceedings of the 1962 Heat Transfer and Fluid Mechanics Institute* (Stanford University Press, Stanford, Calif., 1962).

[13] Szikles, E. A. and Banas, O. M., "Mass transfer cooling in compressible laminar flow"; also Masson, D. J. (comp.), "Mass transfer cooling for hypersonic flight," The Rand Corp., Paper S–51 (June 24, 1957).

[14] Fay, J. A. and Riddell, F. R., "Theory of stagnation point heat transfer," J. Aeronaut. Sci. **24**, 73–85 (February 1958).

[15] Van Driest, E. R., "The problem of aerodynamic heating," Aeronaut. Eng. Rev. **15**, 26–51 (October 1956).